Electronic Supplementary Information

Ultrasmall SnS Nanoparticles Embedded in Carbon Spheres: A High-performance Anode Materials for Sodium Ion Batteries

Jiwei Wang, Yanying Lu, Ning Zhang, Xingde Xiang, Jing Liang* and Jun Chen

Key Laboratory of Advanced Energy Materials Chemistry (Ministry of Education)

Nankai University, Tianjin 300071, China

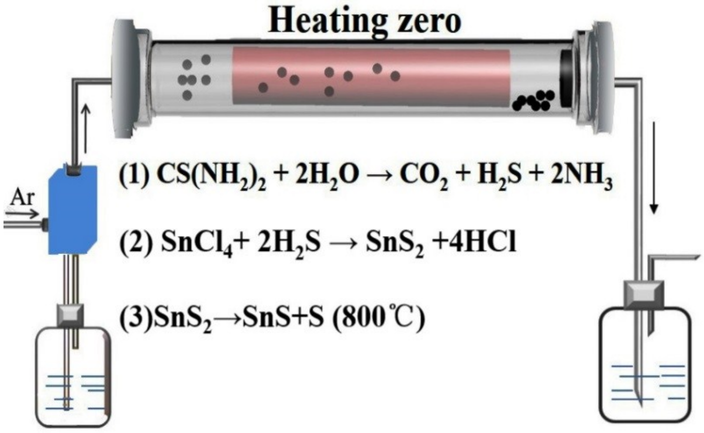

Scheme. 1 Schematic illustration for aerosol spray pyrolysis apparatus and the formation process of SnS/C composite.

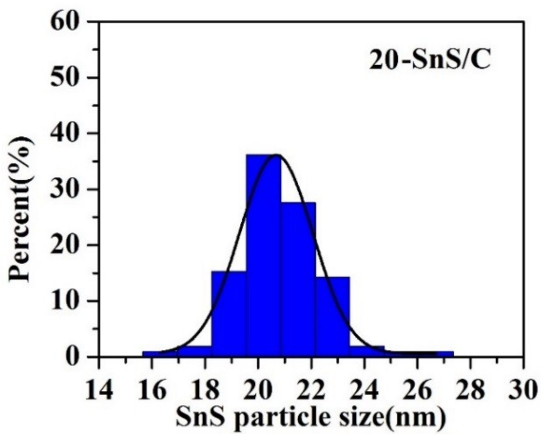

Fig. S1 The distribution pattern of 20-SnS/C nanoparticles.

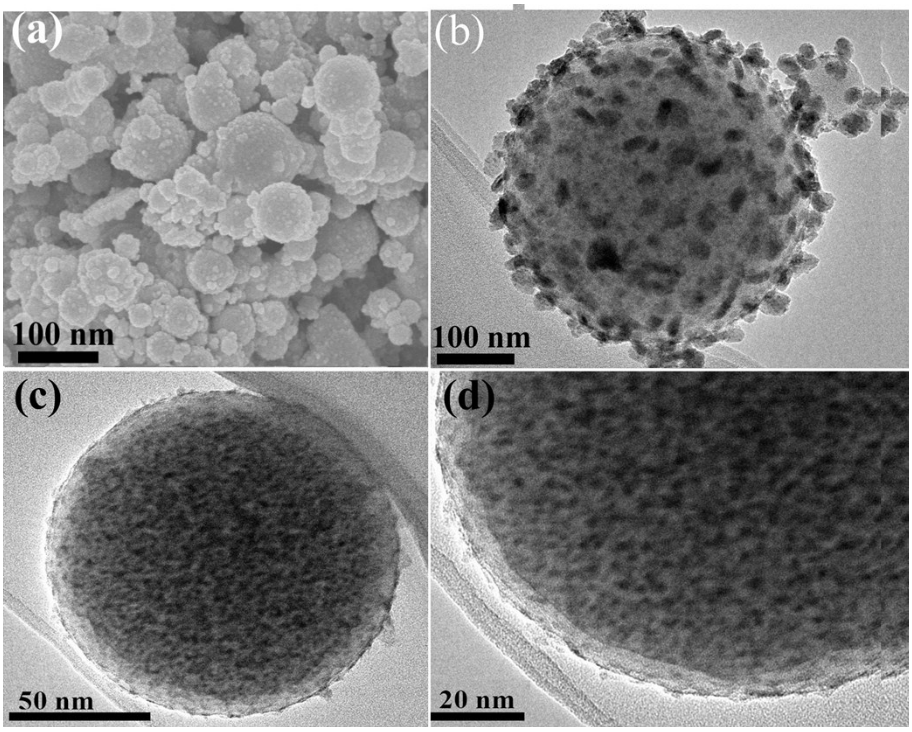

Fig.S2 (a) SEM and (b) TEM images of 20-SnS/C. (c), (d) TEM images of 5-SnS/C embeded in carbon spheres.

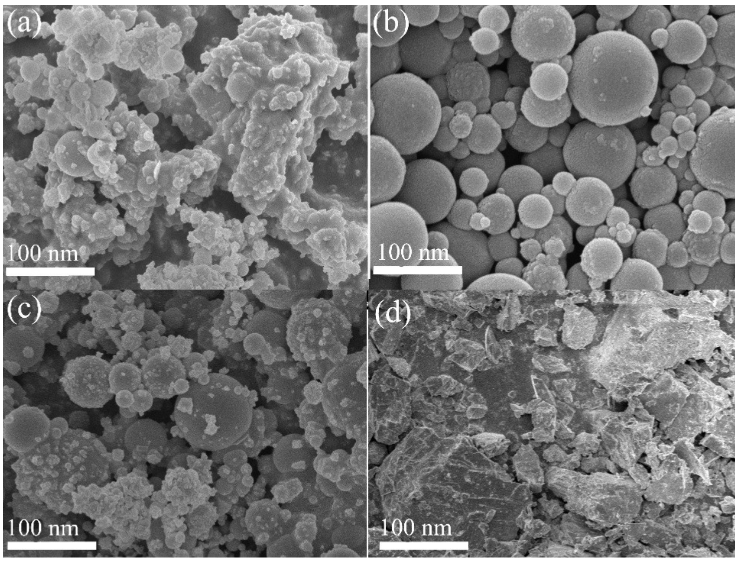

Fig. S3 SEM images of 5-SnS/C with the same precursor solution (0.4M Sn^{4+}) and different reaction temperature of (a) 700 °C, (b) 800 °C, and (c) 900 °C, respectively. (d) SEM image of pure SnS.

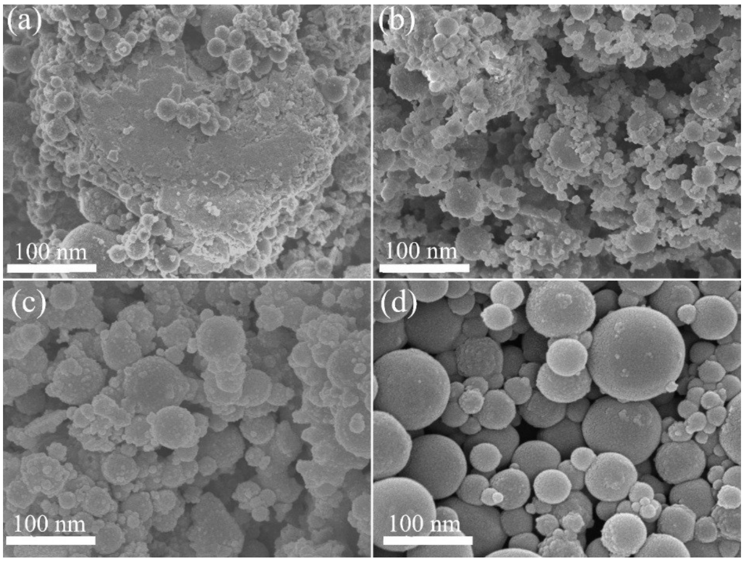

Fig. S4 SEM images of samples at 800℃ with different Sn^{4+} concentration of (a) 0.08M, (b) 0.07M, (c) 0.05M, and (d) 0.04M, respectively.

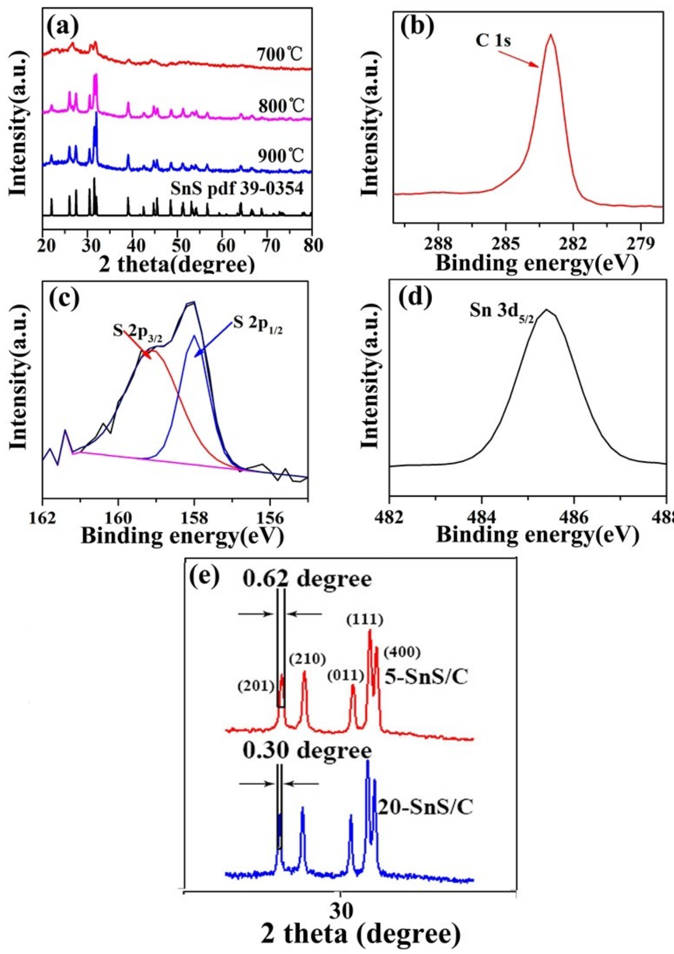

Fig. S5 (a) XRD pattern of 5-SnS/C composite at different synthesize temperature and pure SnS. XPS spectra of (b) C 1s of 5-SnS/C, (c) S 2p of 5-SnS/C and (d) Sn 3d of 5-SnS/C. (e) the full width at half maximum (FWHM) for main peak of (201).

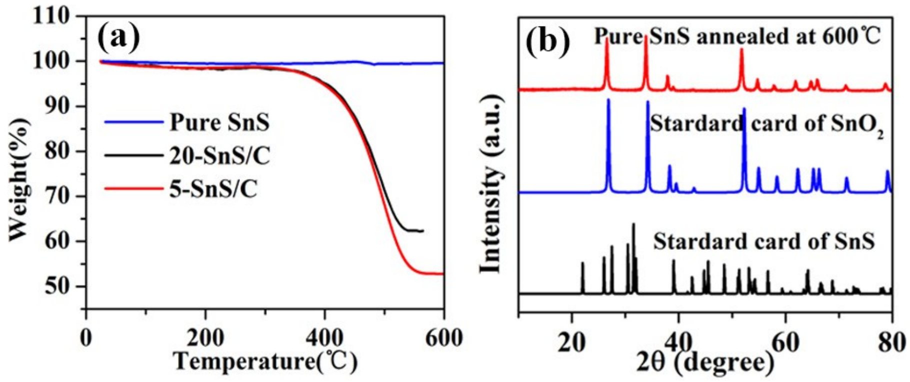

Fig. S6 (a)TGA curve of 5-SnS/C, 20-SnS/C and pure SnS. (b) XRD patterns of pure SnS annealed at 600℃.

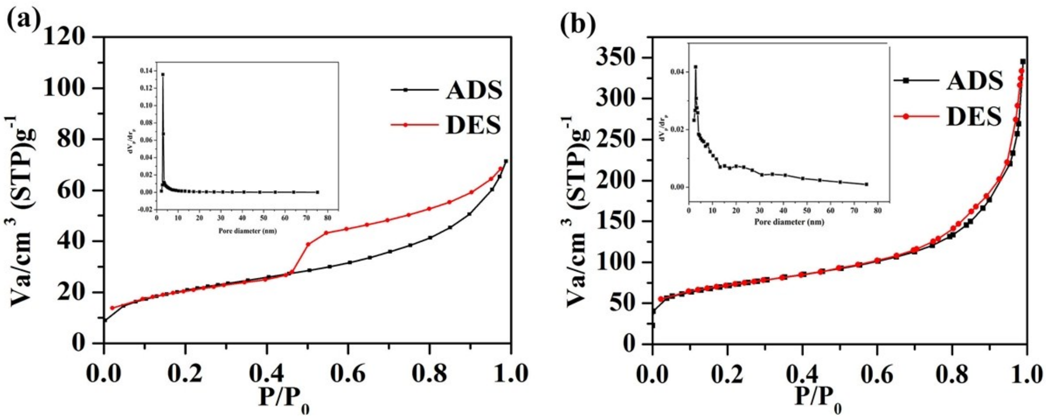

Fig. S7 N_2 adsorption-desorption isotherms of (a) 20-SnS/C and (b) 5-SnS/C. The pore size distribution of 20-SnS/C and 5-SnS/C were inserted in (a) and (b), respectively.

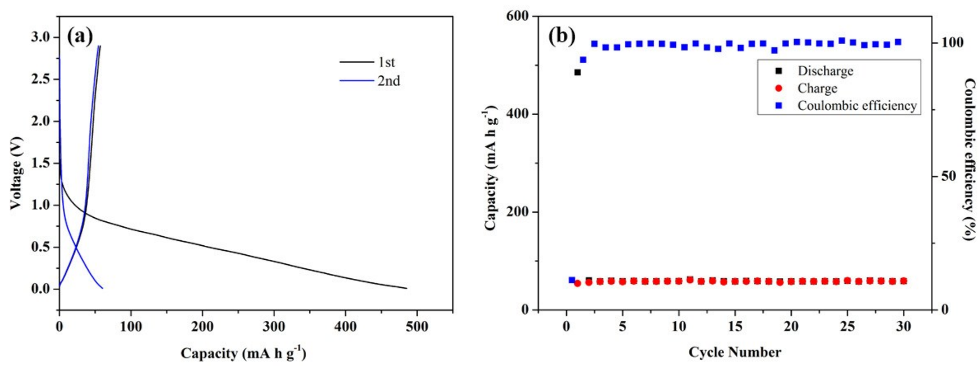

Fig. S8. (a) Galvanostatic discharge/charge curves of pure carbon at 50 mA g^{-1}. (b) Cycling stability and the corresponding coulombic efficiency of pure carbon at 50 mA g^{-1}.

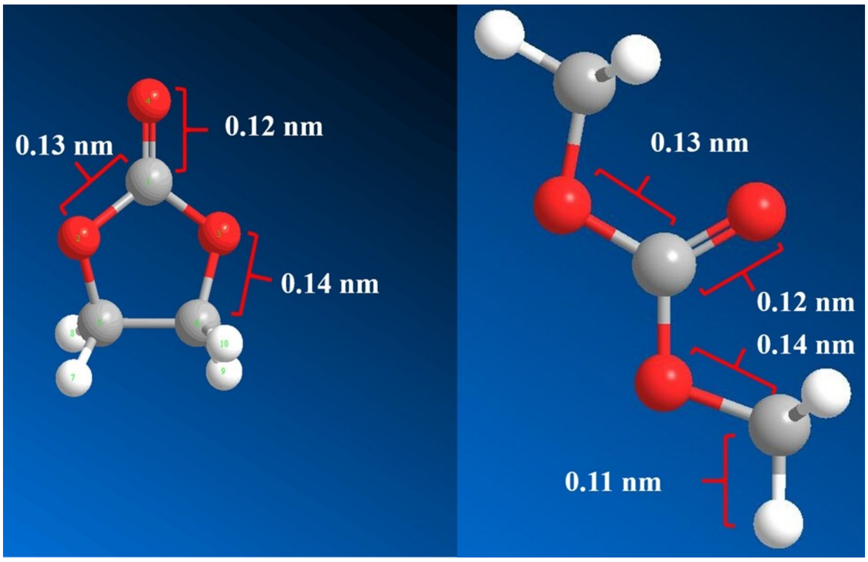

Fig. S9 Molecular structure of the electrolyte EC (ethylene carbonate) and DMC (dimethyl carbonate).

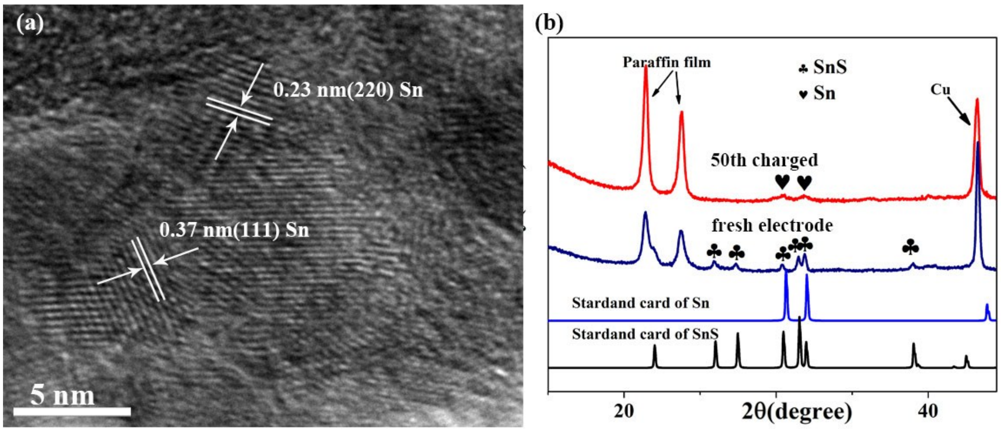

Fig. S10 (a). The HRTEM of charged products for 5-SnS/C composite after 50 cycles. (b) The XRD pattern of 5-SnS/C composite after 50 cycles.

Table. S1 Based on XRD data using the Debye-Scherrer equation: Diameter = 0.89*λ/β*cosθ, where λ is the wavelength of the X-ray (0.154 nm) and β is the full width at half maximum of the diffraction peak. The average size of 5-SnS/C and 20-SnS/C calculated from XRD is 12.9 and 25.8 nm, respectively.

Sample	Index	2θ (degree)	β (degree)	Diameter (nm)
5-SnS/C	(201)	26.08	0.62	12.7
5-SnS/C	(210)	27.48	0.60	13.1
20-SnS/C	(201)	26.05	0.30	26.2
20-SnS/C	(210)	27.44	0.31	25.4

Table. S2 The carbon and hydrogen content of 5-SnS/C and 20-SnS/C composites.

	C	H
5-SnS/C	44.96%	0.31%
20-SnS/C	35.61%	0.55%

Table. S3 The results of our study compared with previously reported performance of SnS-based anodes for SIBs.

Sample	Rate capability	Cyclic stability	Ref.
nano-cubic SnS-C	415 mAh/g at 3 A/g 333 mAh/g at 4 A/g 285 mAh/g at 5 A/g	433 mAh/g at 0.5A/g (50 cycles)	27
SnS nano-rod	390 mAh/g at 0.5 A/g 300 mAh/g at 1 A/g	370 mAh/g at 0.5A/g (30 cycles)	8
SnS/Graphene/Carbon	590 mAh/g at 0.05 A/g 458 mAh/g at 0.5 A/g	510 mAh/g at 0.05A/g (30 cycles)	30
SnS/Graphene	~580 mAh/g at 0.81 A/g ~300 mAh/g at 7.29A/g	492 mAh/g at 0.81A/g (250 cycles)	19
SnS/C	524 mAh/g at 0.2A/g 493 mAh/g at 0.4A/g 452 mAh/g at 0.8A/g	531.6 mAh/g at 0.1A/g (80 cycles)	13
5-SnS/C	428.5 mAh/g at 3A/g 315.4 mAh/g at 5A/g	517.6 mAh/g at 1A/g (200 cycles)	Present work